



Published in final edited form as:

Aging Cell. 2013 February ; 12(1): 130–138. doi:10.1111/ace.12029.

A METABOLIC SIGNATURE FOR LONG-LIFE IN THE *C. ELEGANS* MIT MUTANTS

Jeffrey A. Butler, Robert J. Mishur, Shylesh Bhaskaran, and Shane L. Rea*

Barshop Institute for Longevity and Aging Studies, & the Department of Physiology, University of Texas Health Science Center, San Antonio, TX78240, USA

SUMMARY

Mit mutations that disrupt function of the mitochondrial electron transport chain can, inexplicably, prolong *Caenorhabditis elegans* lifespan. In this study we use a metabolomics approach to identify an ensemble of mitochondrial-derived α -ketoacids and α -hydroxyacids that are produced by long-lived Mit mutants but not by other long-lived mutants or by short-lived mitochondrial mutants. We show that accumulation of these compounds is dependent upon concerted inhibition of three α -ketoacid dehydrogenases that share dihydrolipoamide dehydrogenase (DLD) as a common subunit, a protein previously linked in humans with increased risk of Alzheimer's disease. When the expression of DLD in wild type animals was reduced using RNA interference we observed an unprecedented effect on lifespan - as RNAi dosage was increased lifespan was significantly shortened but, at higher doses, it was significantly lengthened, suggesting DLD plays a unique role in modulating length of life. Our findings provide novel insight into the origin of the Mit phenotype.

Keywords

branched-chain α -keto acids; *clk-1*; *isp-1*; *nuo-6*; *tpk-1*; *mev-1*; *ucr-2.3*

INTRODUCTION

The Mit mutants of *Caenorhabditis elegans* have impaired mitochondrial electron transport chain (ETC) activity yet are long-lived (Rea & Johnson 2003). Several proteins have been identified that *modulate* the longevity response in some or all of the Mit mutants, including HIF-1, p53, CEH-23, CRTC-1, CREB and AMP kinase (Apfeld *et al.* 2004; Ventura *et al.* 2009; Lee *et al.* 2010; Mair *et al.* 2011; Walter *et al.* 2011). In addition, reactive oxygen species (ROS), the mitochondrial unfolded protein response (UPR), and autophagy have also been shown to *modulate* the severity of the Mit phenotype when their level of production or operation is altered (Haynes *et al.* 2007; Lee *et al.* 2010; Yang & Hekimi 2010; Nargund *et al.* 2012). Despite all of these findings, the underlying events that *establish* the Mit

*To whom correspondence should be addressed: Shane L. Rea (Ph.D), Barshop Institute for Longevity and Aging Studies, 15355 Lambda Drive, STCBM Building, Rm. 2.200.04, Texas Research Park, San Antonio, TX 78245-3207, ph: 210 562 5092, fax: 210 562 5028, reas3@uthscsa.edu.

Jeffrey A. Butler: jebutler@vt.edu

Robert J. Mishur: Mishur@uthscsa.edu

Shylesh Bhaskaran: bhaskaran.shylesh@gmail.com

AUTHOR CONTRIBUTIONS:

JAB, RJM and SLR designed the experiments, collected the data, analyzed the data and co-wrote the manuscript. SB also aided in data collection.

phenotype are not known. Moreover, why Mit mutations extend lifespan in worms, while other ETC mutations that also disrupt the ETC chain shorten lifespan, remains unknown.

Recent studies using tissue-specific RNAi knock-down in *C. elegans* have suggested that restricting mitochondrial dysfunction to neuronal or intestinal cells may be sufficient to extend the lifespan of otherwise wild type animals (Durieux *et al.* 2011). These studies have led to the suggestion that a mitokine may emanate from dysfunctional mitochondria to systemically reprogram unaffected cells and increase animal lifespan. The nature of such a signal remains unknown. In this study we identify a set of small metabolites that are uniquely generated by Mit mutants. We identify their enzymatic source and discover the unifying principle behind the Mit phenotype.

RESULTS

GC-MS footprinting defines a Mit mutant-specific metabolic signature

We reasoned that dysfunctional mitochondria may accumulate novel metabolites, or accumulate normal metabolites to abnormal levels, which in turn may serve as systemic signaling molecules. Such molecules might also be expected to become enriched in the external environment. Synchronous populations of the long-lived strain *isp-1(qm150)*, the short-lived strain *mev-1(kn1)*, and wild type animals were generated as previously described (Butler *et al.* 2010), and metabolite excretion monitored over a 20 hour period using GC-MS footprinting (Butler *et al.* 2012). All three strains generated ~100 compounds that we could reliably detect, allowing us to identify compounds whose production over time differed significantly between strains (Figure 1A, Supplementary Figure 1). Metabolites which co-varied over time within each strain were also identified (Supplementary Figures 2-4). A unique feature of *isp-1* Mit mutants was significantly increased production of branched-chain α -ketoacids and their corresponding α -hydroxyacid reduction products (Figure 1A, red asterisks). Increased production of these compounds was also observed in two other long-lived Mit mutants, *clk-1(qm30)* (Wong *et al.* 1995) and *nuo-6(qm200)* (Yang & Hekimi 2010), at levels that distinguished them significantly from wild type animals ($p < 0.005$ and $p < 0.0042$, respectively) (Figure 1B, Supplementary Figures 5-7). In contrast, short-lived *mev-1(kn1)* and *ucr-2.3(pk732)* mutants generated their own unique metabolic signature that was enriched in amino acids and tricarboxylic acid (TCA) cycle intermediates (Figure 1C); a profile that may reflect enhanced flux into the TCA cycle. We next examined whether other long-lived (Age) mutants also generated products similar to those made by Mit mutants. Production of branched chain α -ketoacids and their corresponding reduction products appears unique to Mit mutants since they were not elevated in the exometabolomes of four other long-lived mutants: *daf-2(e1370)*, *clk-2(qm37)*, *eat-2(ad465)* and *slcf-1(tm2258)* (Benard *et al.* 2001; Mouchiroud *et al.* 2011) (Figure 1B & Supplementary Figures 5-7). These findings are consistent with genetic evidence suggesting *daf-2*, *eat-2* and *clk-2* mutants extend lifespan in a manner distinct from, or at best partially overlapping with, that of Mit mutants (Lakowski & Hekimi 1996; Lakowski & Hekimi 1998).

The Mit mutant metabolic profile is distinct from that of anaerobic worms

Several observations have led to the proposition that Mit mutants ectopically activate metabolic pathways normally reserved for survival under low or no oxygen. These observations include enhanced tolerance of Mit mutants to acute anoxia (Butler *et al.* 2010), and the fact that loss of hypoxia-inducible factor-1 (HIF-1) in *isp-1(qm150)* and *clk-1(qm30)* Mit mutants mitigates their increased longevity (Lee *et al.* 2010). We found that Mit mutants do not generate metabolic end products characteristic of wild type worms exposed to anoxic conditions (Supplementary Figures 8 & 9). In particular, excretion of volatile fatty acids, signature molecules of anaerobic worms (Butler *et al.* 2012), is not

observed in Mit mutants grown under normoxic conditions (Supplementary Figure 8A). All Mit mutants nonetheless remain capable of robust volatile fatty acid production when placed under anoxia (Supplementary Figure 8A). Collectively, these data indicate that the mechanisms functioning in Mit mutants to counteract their ETC deficit and extend their health- and life-span are distinct from canonical *C. elegans* anaerobic survival processes, and imply use of a potentially novel metabolism.

DLD inhibition phenocopies the metabolic profile of Mit mutants

Many of the compounds that differentially accumulate in the exometabolome of Mit mutants are related by redox chemistry (Figure 1D). A second feature that unites many of these compounds is the connection of their parent α -ketoacid with the enzyme dihydrolipoamide dehydrogenase. DLD (or E3) is a shared subunit of three evolutionarily related enzyme supercomplexes – branched-chain α -keto acid dehydrogenase (BCKADH), pyruvate dehydrogenase (PDH), and α -ketoglutarate dehydrogenase (α -KGDH) (Kochi *et al.* 1986; Matuda *et al.* 1991). All three enzymes are central components of intermediary metabolism and each acts to oxidatively decarboxylate one or more α -ketoacids. The striking metabolic profile of Mit mutants suggested to us that DLD may be inhibited in these animals. When a feeding RNAi was used to incrementally reduce DLD expression (Bhaskaran *et al.* 2011) in wild type worms (Figure 2A-C), we observed that the excreted metabolic profile that followed the most potent knockdown of DLD (~85%) correlated most closely with that of *nuo-6(qm200)* Mit mutants ($r_{AV} = 0.87$, $n = 7$) (Figures 2D, 3B & Supplementary Figures 10-16).

Graded inhibition of DLD causes a novel effect on lifespan

We have previously shown that RNAi directed against Mit genes in wild type worms reproduces many aspects of the Mit phenotype (Rea *et al.* 2007). We showed that as RNAi dosage was increased, post-embryonic development slowed, adult size became smaller, and adult lifespan was extended. At a critical dose of RNAi these life enhancing properties either plateaued or, for some target genes such as *atp-3*, lifespan reached a pathological turning point beyond which lifespan began to shorten. We tested whether incrementally reducing DLD activity by RNAi also reproduced other aspects of the Mit phenotype. RNAi-mediated inhibition of DLD in wild type worms resulted in slowed development (not quantified) and decreased final adult size (Figure 2E). Unexpectedly, we observed that intermediate doses of DLD RNAi significantly ($p < 0.005$) shortened adult lifespan, while more potent doses of DLD RNAi significantly ($p < 0.005$) extended adult life span (Figure 2F, Supplementary Figure 17). This biphasic effect of gene dosage on longevity has, to the best of our knowledge, never before been reported for any gene and supports our hypothesis that DLD plays a central role in the regulation of aging in Mit mutants.

DLD has a fourth function in cells

DLD not only functions to channel electrons to NAD^+ in the final step of the three α -ketoacid dehydrogenase supercomplexes, it also performs a similar role in the glycine cleavage system (GCS) in which 5,10-methylene-tetrahydrofolate is produced from glycine (Kikuchi *et al.* 2008). Unlike for the α -keto acid dehydrogenases, the ensemble of reactions that comprise the GCS is fully reversible (Kikuchi *et al.* 2008). We noted for wild type worms treated with increasing amounts of RNAi targeting DLD, that their exometabolome accumulated increasing amounts of glycine (Figure 2D). Curiously, for *clk-1(qm30)* and *isp-1(qm150)* Mit mutants, glycine was not a compound that accumulated significantly (Figure 1A, Supplementary Figures 6, 7). For *nuo-6(qm200)* mutants, glycine was elevated significantly (Supplementary Figure 7), but this level paled when compared with that in DLD RNAi-treated animals (Figure 3A). One interpretation of this observation is that DLD activity is not directly inhibited in Mit mutants, leading to the alternate hypothesis that α -

keto acid dehydrogenase supercomplexes are inactivated via DLD-independent mechanisms, possibly at the level of their E1 or E2 subunits. Consistent with this notion, when we assayed DLD enzymatic function in *isp-1(qm150)* Mit mutants, after disrupting the α -keto acid supercomplexes and freeing DLD from bound E1 and E2, we observed no decrease in its activity relative to that of wild type animals (Figure 2G).

Disruption of a positive regulator of α -keto acid dehydrogenases mimics the Mit mutant phenotype

E1 proteins catalyze the irreversible decarboxylation of their α -ketoacid substrate and they are the primary site of α -ketoacid dehydrogenase regulation in mammalian cells. We tested if either individual site or concerted inhibition of these enzymes in wild type worms could phenocopy the longevity of Mit mutants. When E1 proteins were separately targeted for disruption by RNAi, no increase in lifespan was detected (Supplementary Figure 18 A-C). We tested a range of concentrations for each RNAi and observed that, in all cases, lifespan remained either unchanged relative to vector control, or was significantly shortened (Supplementary Figure 18B). Out of the three series, RNAi targeting E1 of α -KGDH had some semblance to DLD RNAi, but no condition extended lifespan significantly. To disrupt all three E1 proteins simultaneously we chose a genetic approach. Thiamine phosphate is an essential co-factor of E1 enzymes (Harris *et al.* 1997), and thiamine phosphorylase is required to phosphorylate and retain thiamine inside cells. *tpk-1(qm162)* mutants contain a hypomorphic disruption in thiamine phosphorylase (de Jong *et al.* 2004). Remarkably, when we analyzed the exometabolome of these mutants (Figure 3A & B, Supplementary Figure 16,) we observed a marked similarity with the exometabolome of *nuo-6(qm200)* Mit mutants (correlation coefficient $r_{AV} = 0.81$, $n = 7$). The *tpk-1(qm162)* profile was also very closely related to the exometabolome profile of long-lived worms treated with undiluted DLD RNAi ($r_{AV} = 0.96$, $n = 3$). *isp-1(qm150)* Mit mutants were also clearly related to *tpk-1(qm162)* mutants by this metric because their correlation coefficient ($r_{AV} = 0.59$, $n = 3$) was still double the next nearest strain's. Across all four strains, we saw marked enrichment of a common set of α -ketoacids and α -hydroxyacids (Figure 1D, E). Remarkably, *tpk-1(qm162)* animals are known to exhibit many Mit-like traits including slowed development, reduced adult size, anoxia tolerance and extended lifespan (de Jong *et al.* 2004; Butler *et al.* 2010). These data suggest that concerted inhibition of the α -ketoacid dehydrogenases is necessary and sufficient to establish the Mit phenotype.

DISCUSSION

In this study we identified an ensemble of α -ketoacids and α -hydroxyacids that are differentially over-produced by Mit mutants. Based on this unique metabolite profile we predicted and showed that DLD, within the context of the α -ketoacid dehydrogenases, was a pivotal control point in the production of these compounds. When we disrupted DLD in wild type worms using RNAi, we made the surprising finding that lifespan was significantly shortened at low RNAi doses but at high RNAi doses it was significantly lengthened. We subsequently discovered that simultaneous disruption of the α -ketoacid dehydrogenases at the level of E1 was necessary and sufficient to recapitulate the Mit phenotype.

Our present findings provide new insight into the genesis of the Mit phenotype. *In vitro* studies show that electrons can be forced to flow backwards into DLD when matrix NADH levels are raised (Starkov *et al.* 2004). In fact, under these conditions, electrons can flow through DLD into E2 to reduce its bound lipoamide cofactor. The reaction catalyzed by E1 is irreversible and so electrons that reside at the level of E2, as dihydrolipoamide, become prone to massive oxidation. When this occurs superoxide is formed, leaving an E2-bound thiyl radical (Starkov *et al.* 2004) that is capable of inactivating the α -keto acid dehydrogenase complex (Bunik & Fernie 2009). Indeed, the superoxide that forms by this

process can be on a scale comparable to that produced by the mitochondrial ETC (Starkov *et al.* 2004). Within this framework a rationale for why some mitochondrial ETC mutations in *C. elegans* increase lifespan while others cause premature death can be proposed: Because both short-lived and long-lived worms containing mitochondrial mutations have elevated ROS levels (Senoo-Matsuda *et al.* 2001; Lee *et al.* 2010), we believe ROS formation is *not* the discriminating factor. Instead, we posit that ETC mutations which increase lifespan are simply ones that allow NADH levels to be raised enough so that electrons can flow backwards into DLD and inhibit the α -keto acid dehydrogenases (Figure 3C). For short-lived ETC mutants, we suggest that their specific mutations either uncouple NADH consumption from ATP production - permitting electrons to leak from the mitochondrial electron transport chain and preventing NADH levels from ever becoming elevated enough to inhibit DLD - or that sufficient amounts of complex I activity remain in these mutants to keep NADH relatively low. Consistent with both ideas, ectopic production of ROS has been recorded in *mev-1* mutants at the level of complex II (Senoo-Matsuda *et al.* 2001); while supercomplexes containing complex I were shown to be specifically decreased in *isp-1(qm150)* mutants, but the spontaneously-derived *isp-1* suppressor mutation *ctb-1(qm189)* functioned to recover these levels (Suthammarak *et al.* 2010). The Mit phenotype is specified before adulthood (Dillin *et al.* 2002; Rea *et al.* 2007). This period of development is a time when even wild type worms are likely to compete with bacteria for local oxygen (Peters *et al.* 1987). We presume matrix NADH levels become critically elevated in Mit mutants during this period.

It is becoming increasingly evident that regular compounds of intermediary metabolism can moonlight as signaling factors to affect cell fate. For example, accrual of succinate following mutation of succinate dehydrogenase (Cervera *et al.* 2009), or of (*R*)-2-hydroxyglutarate following disruption of isocitrate dehydrogenase (Xu *et al.* 2011), both result in oncogenesis. These so-called oncometabolites are thought to act by disrupting hypoxia-inducible factor 1 (HIF-1) and/or the epigenetic landscape of cells; specifically by altering the activity of EGL-9/PHD1-3 prolyl hydroxylases (Koivunen *et al.* 2012), *jmjC*-type histone demethylases and/or TET family 5-methylcytosine (5mC) hydroxylases (McCarthy 2012). New studies have uncovered a more nuanced level of control by 2-hydroxyglutarate: (*R*)-2-HG activates EGL-9/PHD proteins by functioning as a rogue substrate; (*S*)-2-HG instead blocks these proteins by acting as a competitive inhibitor (Koivunen *et al.* 2012). One intriguing possibility is that the α -ketoacids and α -hydroxyacids that accumulate in Mit mutants may act in a similar signaling manner. To this end we note that at least one of the accumulated α -ketoacids, pyruvate, can extend lifespan when supplemented to the diet of wild type worms (Mouchiroud *et al.* 2011). Moreover, several of the compounds that accumulate in Mit mutants are already known to inhibit the same enzymes targeted by the above-mentioned oncometabolites (Figure 1D), including EGL-9 which regulates HIF-1 and is required for Mit mutant life extension (Lu *et al.* 2005; Lee *et al.* 2010). Interestingly, the most potent dose of DLD RNAi that extended lifespan in wild type worms was also the dose associated with the greatest amounts of α -ketoacid and α -hydroxyacid accumulation. Future studies will be aimed at exploring further this hypothesis.

We observed an unprecedented effect of DLD RNAi on nematode lifespan. At this point we can only speculate why lifespan was decreased at intermediate DLD RNAi doses, but was lengthened by more potent RNAi doses. Excluding off-target RNAi effects, one idea pertains to the fact that α -ketoacid dehydrogenases are multimeric assemblages of E1, E2 and DLD subunits (Zhou *et al.* 2001). Perhaps DLD protein levels have to reach a critically low concentration before complexes disassemble fully. If so, electrons fed from the direction of E1 may inadvertently turn these semi-stable complexes into ROS generators as DLD levels become progressively rate-limiting. With full complex disassembly, ROS production

would not be possible, allowing any potentially pro-longevity signal (α -ketoacids and α -hydroxyacids) to dominate the signaling landscape.

Four non-coding SNPs at the DLD locus of humans have been associated with increased risk of late onset Alzheimer's disease in both Caucasian males and in an Ashkenazi Jewish population (Brown *et al.* 2004). Whether these SNPs are associated with reduced DLD activity is unknown, but the biphasic effects of *dld-1* RNAi on lifespan in *C. elegans*, coupled with its impact on exometabolite composition, suggest that mild DLD dysfunction in humans might alter the penetrance of age-related disorders such as Alzheimer's disease, or perhaps even drive mutagenic events that result in cancer.

EXPERIMENTAL PROCEDURES

Caenorhabditis elegans Maintenance

The following *C. elegans* strains were used for this study: N2 Bristol, CB1370 [*daf-2(e1370)III*], DA465 [*eat-2(ad465)II*], MQ125 [*clk-2(qm37)III*], MQ130 [*clk-1(qm30)III*], MQ770 [*tpk-1(qm162)III*], MQ887 [*isp-1(qm150)IV*], MQ1333 [*nuo-6(qm200)I*], NL1832 [*ucr-2.3(pk732)III*], SLR0032 [*mev-1(kn1)III*], SP506 [*rad-5(mn159)III*], TJ564_{Bx1} [*isp-1(qm150)IV;(gst-4::gfp)III*], TJ5032 [*clk-1(qm30)III;(gst-4::gfp)III*], TK22 [*mev-1(kn1)III*] and TM2285 [*slcf-1(tm2285)X*]. All strains were maintained at 20°C, on NGM agar plates containing lawns of *E. coli* (OP50), using standard worm culture techniques (Wood 1988).

Feeding RNAi

All feeding RNAi constructs were obtained from the Ahringer RNAi library (Kamath & Ahringer 2003). Targeted genes included: DLD, BCKADH E1 α , PDH E1 α , and α -KGDH E1 corresponding to RNAi clones JA:LLC3.1, JA:Y39E4A.3, JA:T05H10.6 and JA:T22B11.5, respectively. All constructs were sequence confirmed. Feeding RNAi, RNAi dilution testing, and lifespan analyses were performed and analyzed exactly as previously described (Rea *et al.* 2007).

Exometabolome Collection

We have described elsewhere detailed methods for exometabolome collection from *C. elegans* cultured under aerobic or anaerobic conditions (Butler *et al.* 2010; Butler *et al.* 2012). In the present studies we utilized 120,000 one-day-old gravid adult worms per replicate. Data for all strains was collected from multiple independent experimental replicates. Briefly, 120,000 arrested L1 larvae were cultured on 12 \times 10-cm BNGM agar plates spread with *E. coli* (OP50). BNGM agar plates consisted of 1% w/v peptone, 2% w/v agar, 50 mM NaCl, 1 mM CaCl₂, 1 mM MgSO₄, 25 mM phosphate, and 5 μ g/mL cholesterol. When animals became gravid adults they were collected in S-Basal (100 mM NaCl, 50 mM KH₂PO₄, pH 6.8), washed extensively in the same buffer (6 \times 50ml), stripped of residual bacteria by sucrose flotation (Foll *et al.* 1999), then again washed extensively in S-Basal (3 \times 15ml). Worm pellets were resuspended in S-Basal to a final concentration of 1 mg/ml. 1.2 ml of worm slurry was then transferred into a 3cm glass dish and rotated (100rpm) for the relevant length of time after which the supernatant containing the worm exometabolome was filtered (0.2 μ m, Life Science Products, Cat #6502-413X) and retained at -80°C until further use.

Multiple strains containing the same mutation were tested when possible to discount background effects. Strains used to generate GC-MS datasets were as follows:

Figure 1A: N2 Bristol, MQ887, SLR0032

Figure 1B: N2 Bristol, TJ564_{Bx1}, MQ1333, TM2285, TK22, CB1370, DA465

Figure 1C & Supplementary Figure 6: N2 Bristol, NL1832, SP506, TJ5032, TJ564_{Bx1}, TK22

Figure 2D: N2 Bristol

Figure 3A: N2 Bristol, MQ770, MQ887, MQ1333, SLR0032

Supplementary Figure 8: N2 Bristol, TJ564_{Bx1}, MQ130, MQ1333, SLR0032, NL1832

GC-MS Acquisition

Aliquots of relevant worm supernatants (100 μ l), were evaporated overnight using vacuum centrifugation. Excreted worm metabolites were then derivitized using methoxyamine HCl (Sigma Aldrich, Cat. No. 226904) and *N*-methyl-*N*-(*tert*-butyldimethylsilyl)trifluoroacetamide containing 1% *tert*-butyldimethylchlorosilane (Thermo Scientific, Cat. No. TS-48927).

GC-MS analyses were undertaken using either an ion-trap (University of Colorado, Boulder, CO) or a quadrupole (University of Texas Health Science Center, San Antonio, TX) mass spectrometer, with an electron impact ionization source. GC separation was performed using a ZB-5MS column (5%-phenyl-arylene 95%-dimethylpolysiloxane), 30 m \times 0.25 mm, 0.25 μ m film thickness (Phenomenex; Torrance CA). MS analyses performed at the UT Health Science Center were conducted on a TRACE DSQ single quadrupole mass spectrometer (Thermo Fisher, San Jose, CA). GC conditions for standard exometabolome samples (UT) were as follows: carrier gas, helium; linear velocity, 1 mL/min (constant flow); injection, split, 10 mL/min split flow; injector temperature, 220 $^{\circ}$ C; column temperature program, initial temperature of 70 $^{\circ}$ C held for 1 min followed by an increase to 310 $^{\circ}$ C at 5 $^{\circ}$ C/min. MS conditions were: ionization, electron impact (70 eV); detection, positive ion; full scan analyses, *m/z* 50 - *m/z* 700 at two scans/sec. Volatile metabolites eluted with the solvent front using this method, so GC separation of these analytes started with an initial temperature of 50 $^{\circ}$ C held for 1 min, followed by an increase to 80 $^{\circ}$ C at 10 $^{\circ}$ C/min. The temperature was maintained for 3 min at 80 $^{\circ}$ C after which it was increased to 275 $^{\circ}$ C at a rate of 30 $^{\circ}$ C/min.

Samples acquired at University of Colorado were analyzed on a Finnigan Polaris Q ion trap (Thermo Fisher, San Jose, CA). Injections onto the GC were performed manually using a hot needle injection technique with 1 μ l of sample sandwiched between two cushions of air in the syringe body. The inlet temperature was 230 $^{\circ}$ C with split ratio of 1:10. Chromatographic conditions were: 1 ml/min constant helium flow with an initial oven temperature of 70 $^{\circ}$ C held for 5 minutes followed by a ramp to 310 $^{\circ}$ C at 5 $^{\circ}$ C min⁻¹ with a final hold of 1 minute. The transfer line was kept at 250 $^{\circ}$ C and the source was operated at 200 $^{\circ}$ C and 70 eV. Masses were scanned from 50-650 *m/z* at \sim 2 scans sec⁻¹. Data acquisition was performed using *Xcalibur* (Thermo Fisher, San Jose, CA).

MS Data Analysis

Peak Integration—Following data acquisition, gas chromatograms were deconvoluted using *AMDIS* (Stein 1999), then extracted ion chromatograms were integrated using *MET-IDEA* (Broeckling et al. 2006). Peak data was sequentially normalized to total worm protein content, and then to the peak area of an exogenously added internal standard (3,4-dimethoxybenzoate). Protein analyses were performed using the bicinchoninic acid-based protein assay (Pierce, Rockford, IL).

Cluster Analysis—Clustering was performed using the Hierarchical Clustering module of the GenePattern software suite (<http://www.broad.mit.edu/cancer/software/genepattern/>) (Reich et al. 2006). Metabolites were clustered using the pairwise complete-linkage method. Distance measures were calculated using Pearson's correlation coefficient. Low abundance and noisy peaks were removed from the analysis prior to clustering. For Figure 1C & Supplementary Figure 6, clustering was performed using the rank orders of metabolite intensities.

SOM—Time course data was analyzed using the self-organizing map (SOM) algorithm of Mayday (<http://microarray-analysis.org/>) (Dietzsch *et al.* 2006). Prior to analysis, data was Z-score transformed (mean centered and scaled by standard deviation). Mayday settings were as follows: cycles, 250; Kernel function, Gaussian; Initial kernel radius, 2.0; Final kernel radius, 0.1; initializer of the SOM-units, random data point; distance measure, Euclidean. The grid topology and number of clusters were altered heuristically until a satisfactory result was obtained. Cluster quality was assessed by silhouette plots.

Significance Testing—To identify metabolites that differed significantly between strains (or groups of strains), normalized GC-MS peak areas were generally rank-ordered across all relevant cases and then analyzed using a General Linear Model (GLM). No effort was made to control for variation in experimenter or sample collection date, but data collected on different MS instruments was segregated. Specific details of all comparisons are provided in the legends of relevant Supplementary Figure files. Contrast coding was performed using SPSS 17.0 (IBM). In all instances significance thresholds were Bonferroni-corrected to adjust for the number of contrasts interrogated.

Quantification of Metabolites

Absolute levels of pyruvate, 2-ketobutyrate, 2-ketoisocaproate, lactate, 2-hydroxybutyrate, 3-hydroxypropionate, 3-hydroxybutyrate, and 2-hydroxycaproate, present in the exometabolome of N2, MQ887 [*isp-1(qm150)*] and MQ1333 [*nuo-6(qm200)*] animals, were determined by comparison to standard curves. Solutions of metabolites of interest were prepared at a range of concentrations (1, 10, 50, 100 and 250 μ M) and analyzed by GC-MS. Data presented in Figure 2G represents averages from multiple independent test samples - N2 (n = 4), MQ1333 (n = 3), and MQ887 (n=7).

Western Blotting

Protein lysates and western analyses were collected and performed, respectively, exactly as described previously (Bhaskaran *et al.* 2011). DLD was analyzed using a rabbit polyclonal antibody raised against native pig heart DLD (1:5000, Abnova, Cat # PAB10259). β -actin was used as a loading control and was analyzed using a mouse monoclonal antibody (1:2000, Sigma, Cat # A5441).

DLD Activity Assay

DLD activity in whole-worm extracts was determined spectrophotometrically, exactly as we have previously described (Bhaskaran *et al.* 2011).

Supplementary Material

Refer to Web version on PubMed Central for supplementary material.

Acknowledgments

We thank Drs. Shawn Ahmed (UNC, Chapel Hill), Benjamin Eaton, Kathleen Fischer, Milena Girotti, and Gregory Macleod (UTHSCSA, San Antonio) for critical reading of the manuscript. Mass spectrometry analyses were conducted in the Institutional Mass Spectrometry Laboratory at UTHSCSA. Technical support was provided by Yvonne Penrod, Adwitiya Kar, Melissa Little and Meghan Cain. Financial support was provided by the National Institute on Aging (RJM & SLR), and the Ellison Medical Foundation (SLR).

REFERENCES

- Apfeld J, O'Connor G, McDonagh T, DiStefano PS, Curtis R. The AMP-activated protein kinase AAK-2 links energy levels and insulin-like signals to lifespan in *C. elegans*. *Genes Dev.* 2004; 18:3004–3009. [PubMed: 15574588]
- Benard C, McCright B, Zhang Y, Felkai S, Lakowski B, Hekimi S. The *C. elegans* maternal-effect gene *clk-2* is essential for embryonic development, encodes a protein homologous to yeast Tel2p and affects telomere length. *Development.* 2001; 128:4045–4055. [PubMed: 11641227]
- Bhaskaran S, Butler JA, Becerra S, Fassio V, Girotti M, Rea SL. Breaking *Caenorhabditis elegans* the easy way using the Balch homogenizer: an old tool for a new application. *Analytical Biochemistry.* 2011; 413:123–132. [PubMed: 21354098]
- Broeckling CD, Reddy IR, Duran AL, Zhao X, Sumner LW. MET-IDEA: data extraction tool for mass spectrometry-based metabolomics. *Anal Chem.* 2006; 78:4334–4341. [PubMed: 16808440]
- Brown AM, Gordon D, Lee H, Caudy M, Hardy J, Haroutunian V, Blass JP. Association of the dihydrolipoamide dehydrogenase gene with Alzheimer's disease in an Ashkenazi Jewish population. *Am J Med Genet B Neuropsychiatr Genet.* 2004; 131B:60–66. [PubMed: 15389771]
- Bunik VI, Fernie AR. Metabolic control exerted by the 2-oxoglutarate dehydrogenase reaction: a cross-kingdom comparison of the crossroad between energy production and nitrogen assimilation. *Biochem J.* 2009; 422:405–421. [PubMed: 19698086]
- Butler JA, Mishur RJ, Bokov AF, Hakala KW, Weintraub ST, Rea SL. Profiling the Anaerobic Response of *C. elegans* Using GC-MS. *PLoS ONE.* 2012; 7:e46140. [PubMed: 23029411]
- Butler JA, Ventura N, Johnson TE, Rea SL. Long-lived mitochondrial (Mit) mutants of *Caenorhabditis elegans* utilize a novel metabolism. *FASEB J.* 2010; 24:4977–4988. [PubMed: 20732954]
- Cervera AM, Bayley JP, Devilee P, McCreath KJ. Inhibition of succinate dehydrogenase dysregulates histone modification in mammalian cells. *Molecular Cancer.* 2009; 8:89. [PubMed: 19849834]
- de Jong L, Meng Y, Dent J, Hekimi S. Thiamine Pyrophosphate Biosynthesis and Transport in the Nematode *Caenorhabditis elegans*. *Genetics.* 2004; 168:845–854. [PubMed: 15514058]
- Dietzsch J, Gehlenborg N, Nieselt K. Mayday—a microarray data analysis workbench. *Bioinformatics.* 2006; 22:1010–1012. [PubMed: 16500939]
- Dillin A, Hsu A-L, Arantes-Oliveira N, Lehrer-Graiwer J, Hsin H, Fraser AG, Kamath RS, Ahringer J, Kenyon C. Rates of Behavior and Aging Specified by Mitochondrial Function During Development. *Science.* 2002; 298:2398–2401. [PubMed: 12471266]
- Durieux J, Wolff S, Dillin A. The Cell-Non-Autonomous Nature of Electron Transport Chain-Mediated Longevity. *Cell.* 2011; 144:79–91. [PubMed: 21215371]
- Foll RL, Pleyers A, Lewandovski GJ, Wermter C, Hegemann V, Paul RJ. Anaerobiosis in the nematode *Caenorhabditis elegans*. *Comp Biochem Physiol B Biochem Mol Biol.* 1999; 124:269–280. [PubMed: 10631804]
- Harris RA, Hawes JW, Popov KM, Zhao Y, Shimomura Y, Sato J, Jaskiewicz J, Hurley TD. Studies on the regulation of the mitochondrial alpha-ketoacid dehydrogenase complexes and their kinases. *Adv Enzyme Regul.* 1997; 37:271–293. [PubMed: 9381974]
- Haynes CM, Petrova K, Benedetti C, Yang Y, Ron D. ClpP Mediates Activation of a Mitochondrial Unfolded Protein Response in *C. elegans*. *Dev. Cell.* 2007; 13:467–480. [PubMed: 17925224]
- Kamath RS, Ahringer J. Genome-wide RNAi screening in *Caenorhabditis elegans*. *Methods.* 2003; 30:313–321. [PubMed: 12828945]
- Kikuchi G, Motokawa Y, Yoshida T, Hiraga K. Glycine cleavage system: reaction mechanism, physiological significance, and hyperglycinemia. *Proc Jpn Acad Ser B Phys Biol Sci.* 2008; 84:246–263.

- Kochi H, Seino H, Ono K. Inhibition of glycine oxidation by pyruvate, alphaketoglutarate, and branched-chain alpha-keto acids in rat liver mitochondria: presence of interaction between the glycine cleavage system and alpha-keto acid dehydrogenase complexes. *Arch Biochem Biophys.* 1986; 249:263–272. [PubMed: 3753002]
- Koivunen P, Lee S, Duncan CG, Lopez G, Lu G, Ramkissoon S, Losman JA, Joensuu P, Bergmann U, Gross S, Travins J, Weiss S, Looper R, Ligon KL, Verhaak RG, Yan H, Kaelin WG Jr. Transformation by the (R)-enantiomer of 2-hydroxyglutarate linked to EGLN activation. *Nature.* 2012; 483:484–488. [PubMed: 22343896]
- Lakowski B, Hekimi S. Determination of life-span in *Caenorhabditis elegans* by four clock genes. *Science.* 1996; 272:1010–1013. [PubMed: 8638122]
- Lakowski B, Hekimi S. The genetics of caloric restriction in *Caenorhabditis elegans*. *Proc Natl Acad Sci U S A.* 1998; 95:13091–13096. [PubMed: 9789046]
- Lee SJ, Hwang AB, Kenyon C. Inhibition of Respiration Extends *C. elegans* Life Span via Reactive Oxygen Species that Increase HIF-1 Activity. *Curr Biol.* 2010; 20:2131–2136. [PubMed: 21093262]
- Lu H, Dalgard CL, Mohyeldin A, McFate T, Tait AS, Verma A. Reversible inactivation of HIF-1 prolyl hydroxylases allows cell metabolism to control basal HIF-1. *The Journal of biological chemistry.* 2005; 280:41928–41939. [PubMed: 16223732]
- Mair W, Morante I, Rodrigues AP, Manning G, Montminy M, Shaw RJ, Dillin A. Lifespan extension induced by AMPK and calcineurin is mediated by CRTC-1 and CREB. *Nature.* 2011; 470:404–408. [PubMed: 21331044]
- Matuda S, Nakano K, Ohta S, Saheki T, Kawanishi Y, Miyata T. The alpha-ketoacid dehydrogenase complexes. Sequence similarity of rat pyruvate dehydrogenase with *Escherichia coli* and *Azotobacter vinelandii* alpha-ketoglutarate dehydrogenase. *Biochim Biophys Acta.* 1991; 1089:1–7. [PubMed: 2025639]
- McCarthy N. Metabolism: unmasking an oncometabolite. *Nat Rev Cancer.* 2012; 12:229. [PubMed: 22378191]
- Mouchiroud L, Molin L, Kasturi P, Triba MN, Dumas ME, Wilson MC, Halestrap AP, Roussel D, Masse I, Dalliere N, Segalat L, Billaud M, Solari F. Pyruvate imbalance mediates metabolic reprogramming and mimics lifespan extension by dietary restriction in *Caenorhabditis elegans*. *Aging Cell.* 2011; 10:39–54. [PubMed: 21040400]
- Nargund AM, Pellegrino MW, Fiorese CJ, Baker BM, Haynes CM. Mitochondrial import efficiency of ATFS-1 regulates mitochondrial UPR activation. *Science.* 2012; 337:587–590. [PubMed: 22700657]
- Peters AC, Wimpenny JW, Coombs JP. Oxygen profiles in, and in the agar beneath, colonies of *Bacillus cereus*, *Staphylococcus albus* and *Escherichia coli*. *Journal of general microbiology.* 1987; 133:1257–1263. [PubMed: 3116170]
- Rea S, Johnson TE. A metabolic model for life span determination in *Caenorhabditis elegans*. *Dev Cell.* 2003; 5:197–203. [PubMed: 12919672]
- Rea SL, Ventura N, Johnson TE. Relationship Between Mitochondrial Electron Transport Chain Dysfunction, Development, and Life Extension in *Caenorhabditis elegans*. *PLoS Biol.* 2007; 5:e259. [PubMed: 17914900]
- Reich M, Liefeld T, Gould J, Lerner J, Tamayo P, Mesirov JP. GenePattern 2.0. *Nat Genet.* 2006; 38:500–501. [PubMed: 16642009]
- Senoo-Matsuda N, Yasuda K, Tsuda M, Ohkubo T, Yoshimura S, Nakazawa H, Hartman PS, Ishii N. A Defect in the Cytochrome b Large Subunit in Complex II Causes Both Superoxide Anion Overproduction and Abnormal Energy Metabolism in *Caenorhabditis elegans*. *J. Biol. Chem.* 2001; 276:41553–41558. 10.1074/jbc.M104718200. [PubMed: 11527963]
- Starkov AA, Fiskum G, Chinopoulos C, Lorenzo BJ, Browne SE, Patel MS, Beal MF. Mitochondrial {alpha}-Ketoglutarate Dehydrogenase Complex Generates Reactive Oxygen Species. *J. Neurosci.* 2004; 24:7779–7788. 10.1523/JNEUROSCI.1899-04.2004. [PubMed: 15356189]
- Stein SE. An integrated method for spectrum extraction and compound identification from gas chromatography/mass spectrometry data. *Journal of the American Society for Mass Spectrometry.* 1999; 10:770–781.

- Suthammarak W, Morgan PG, Sedensky MM. Mutations in mitochondrial complex III uniquely affect complex I in *Caenorhabditis elegans*. *J Biol Chem*. 2010; 285:40724–40731. [PubMed: 20971856]
- Ventura N, Rea SL, Schiavi A, Torgovnick A, Testi R, Johnson TE. p53/CEP-1 increases or decreases lifespan, depending on level of mitochondrial bioenergetic stress. *Aging Cell*. 2009; 8:380–393. [PubMed: 19416129]
- Walter L, Baruah A, Chang HW, Pace HM, Lee SS. The homeobox protein CEH-23 mediates prolonged longevity in response to impaired mitochondrial electron transport chain in *C. elegans*. *PLoS Biology*. 2011; 9:e1001084. [PubMed: 21713031]
- Wong A, Boutis P, Hekimi S. Mutations in the *clk-1* Gene of *Caenorhabditis elegans* Affect Developmental and Behavioral Timing. *Genetics*. 1995; 139:1247–1259. [PubMed: 7768437]
- Wood, WB. *The Nematode Caenorhabditis elegans* (eds). Cold Spring Harbor Laboratory; New York: 1988. p. 667
- Xu W, Yang H, Liu Y, Yang Y, Wang P, Kim SH, Ito S, Yang C, Xiao MT, Liu LX, Jiang WQ, Liu J, Zhang JY, Wang B, Frye S, Zhang Y, Xu YH, Lei QY, Guan KL, Zhao SM, Xiong Y. Oncometabolite 2-Hydroxyglutarate Is a Competitive Inhibitor of alpha-Ketoglutarate-Dependent Dioxygenases. *Cancer Cell*. 2011; 19:17–30. [PubMed: 21251613]
- Yang W, Hekimi S. Two modes of mitochondrial dysfunction lead independently to lifespan extension in *Caenorhabditis elegans*. *Aging Cell*. 2010
- Zhou ZH, McCarthy DB, O'Connor CM, Reed LJ, Stoops JK. The remarkable structural and functional organization of the eukaryotic pyruvate dehydrogenase complexes. *Proc Natl Acad Sci U S A*. 2001; 98:14802–14807. [PubMed: 11752427]

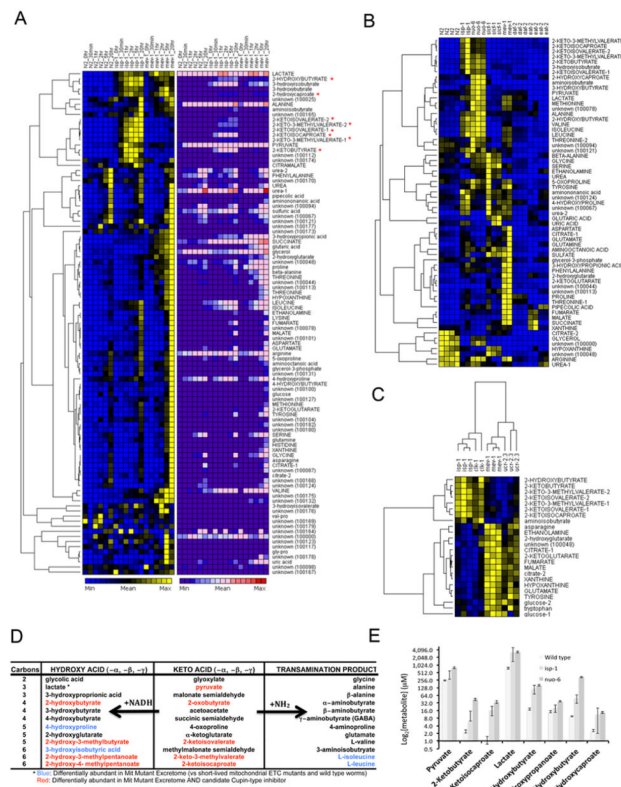


Figure 1. A metabolic signature for long-life in the *C. elegans* Mit mutants

(A) Exometabolome analysis of wild type worms (N2), *isp-1(qm150)* and *mev-1(kn1)* mutants: 120,000 worms were transferred to minimal media and their exometabolome sampled over a 20 hr period (at +0, 0.5, 1, 2, 5, 20 hr). GC-MS was used to identify and quantify metabolites within each sample. Data is presented using hierarchical clustering (Pearson's correlation coefficient): *left panel*, metabolite variation across row; *right panel*, metabolite variation relative to the entire array. Asterisks mark several α -ketoacids and α -hydroxyacids that are significantly overproduced by *isp-1* mutants (statistical analyses summarized in Supplementary Figure 1). (B, C) Exometabolome analysis of various Mit, Age and short-lived mutants. Data was collected as described in (A) following an 18 hr metabolite capture period. Results are presented as in the left panel of A. In (C) only metabolites that differed significantly ($p < 0.0062$) between long-lived and short-lived ETC mutants are shown (full results are provided in Supplementary Figures 6 & 7). Strains are marked at the top of each panel. (D) Many of the compounds detected in the exometabolome of worms strains are related by redox reactions. Metabolites that are specifically enriched in the exometabolome of Mit mutants are highlighted. (E) Quantification of select α -ketoacids and α -hydroxyacids in the +18 hr exometabolome of wild type (N2), *isp-1(qm150)* and *nuo-6(qm200)* animals. Ordinate is plotted on a *log scale*.

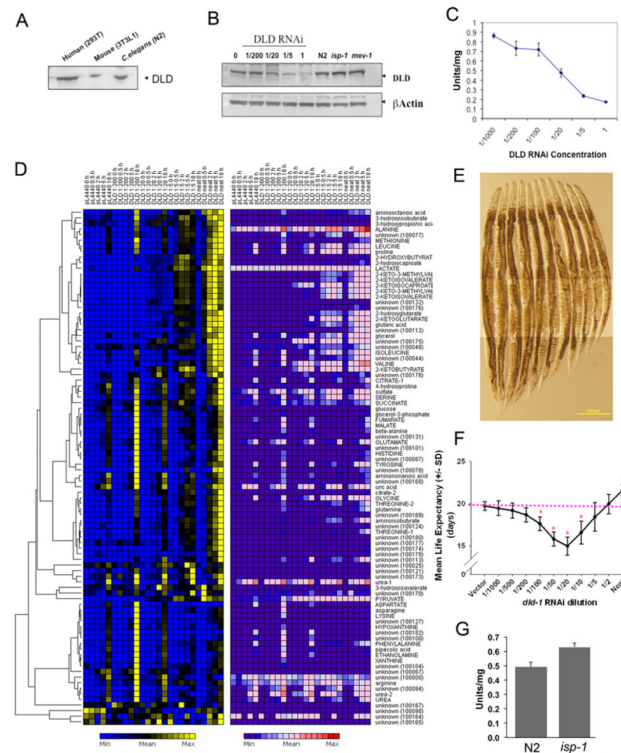


Figure 2. Inhibition of dihydrolipoamide dehydrogenase activity leads to metabolic and phenotypic recapitulation of the Mit phenotype

(A, B) Cross-reactivity of α -DLD polyclonal antibody with human (HEK293T) and mouse (3T3-L1 fibroblast) whole-cell extracts, and with whole-worm extracts of N2, *isp-1(qm150)* and *mev-1(kn1)*. Also tested in (B) were whole-worm extracts from a feeding RNAi dilution series (Rea *et al.* 2007) targeting DLD (RNAi to empty vector ratio - 0:1, 1:200, 1:20, 1:5, and 1:0). Animals were fed DLD RNAi from the time of hatching. All lanes contain 25 μ g of protein; β -actin served as loading control in (B). (C) DLD activity in whole-worm extracts from two independently-collected DLD feeding RNAi dilution series. One unit of DLD activity is defined as the rate of production of 1 μ mol of NADH in 1 min at 25°C (Bhaskaran *et al.* 2011) (error bars: \pm SD). (D) Temporal changes in the exometabolome of N2 worms following treatment with increasing amounts of DLD RNAi (RNAi to empty vector ratio - 0:1, 1:200, 1:20, 1:5, and 1:0). Excreted metabolites were collected at +0, 0.5, 2, 5 and 18 hr. Data was analyzed by GC-MS and is presented using hierarchical clustering – *left panel*, metabolite variation across row; *right panel*, metabolite variation relative to the entire array. (See also Supplementary Figures 10-15). (E, F) Increasing doses of RNAi targeting DLD (RNAi to empty vector ratio - 0:1, 1:1000, 1:500, 1:200, 1:100, 1:50, 1:20, 1:10, 1:5, 1:2 and 1:0) were fed to wild type *C. elegans* from the time of hatching and the effects on both adult size (E, Scale bar: 200 μ m) and lifespan (F) measured. Lifespan data is the mean of four replicates (\pm) S.E.M. (n = 60 worms/condition/replicate; asterisks indicates significantly different from vector, $p < 0.005$ (Bonferroni corrected), summary statistics are tabulated in Supplementary Figure 17). (G) DLD activity in whole-worm extracts from N2 and *isp-1(qm150)* animals (n = 3 replicates, error bars: \pm SD).

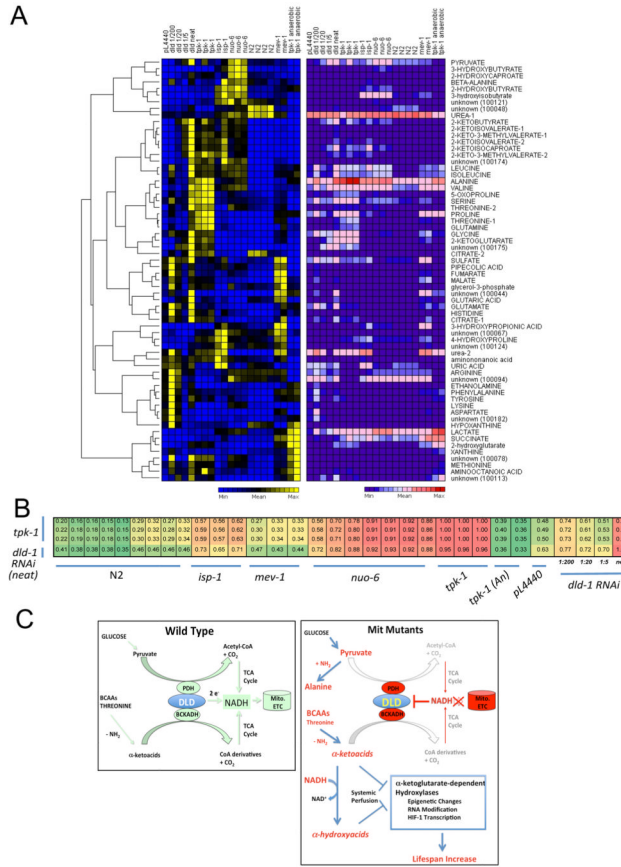


Figure 3. Exometabolome analysis of *tpk-1(qm162)* mutants reveals concerted inhibition of α -ketoacid dehydrogenase activity is sufficient to recapitulate the Mit metabolic phenotype
(A) The +18 hr exometabolome of the following strains were collected and analyzed by GC-MS: wild type worms (N2), *isp-1(qm150)* and *nuo-6(qm200)* Mit mutants, short-lived *mev-1(kn1)* mutants, N2 exposed to DLD RNAi from the time of hatching (RNAi to vector ratios of 0:1, 1:200, 1:20, 1:5, and 1:0), and *tpk-1(qm162)* mutants exposed for 18 hours to both normoxia or anoxia. Columns represent independent experimental replicates. Data is presented using hierarchical clustering – *left panel*, metabolite variation across row; *right panel*, metabolite variation relative to the entire array. Statistical analyses are summarized in Supplementary Figures 5. See also Supplementary Figure 16 for global correlation analysis.
(B) Correlation matrix showing metabolic similarity between +18 hr exometabolome of long-lived Mit mutants, long-lived *dld-1* disrupted animals, and long-lived *tpk-1(qm162)* mutants. Details of distance measure calculations are described in Supplementary Figure 16.
(C) Model for the genesis of the Mit phenotype (BCAA - branched chain amino acids; Mito. ETC – mitochondrial electron transport chain).